Eur. Phys. J. Appl. Phys. **53**, 10601 (2011)
DOI: 10.1051/epjap/2010100095

THE EUROPEAN PHYSICAL JOURNAL APPLIED PHYSICS

Regular Article

Synthesis and characterization of pure and zinc doped calcium pyrophosphate dihydrate nanoparticles

S.R. Vasant[a] and M.J. Joshi

Crystal Growth Laboratory, Physics Department, Saurashtra University, Rajkot 360 005, Gujarat, India

Received: 5 March 2010 / Accepted: 27 September 2010
Published online: 23 December 2010 –

Abstract. Calcium phosphate based biomaterials are widely used in dentistry and as a bone substitutes in orthopedic applications. Calcium pyrophosphate (CPP) – a type of calcium phosphate and a shortest linear polyphosphate can also be used as a bone graft. Successive applications of theses materials depend on the degree of bio-resorption, mechanical strength and bio-compatibility. Zinc improves the bone activity of osteoblast, promotes the bone regeneration and also stimulates enzyme activity. In the present study Zn doped calcium pyrophosphate dihydrate (Zn-CPPD) nanoparticles were synthesized using surfactant mediated approach with varying [Zn]/[Ca] molar ratio as 0% (pure CPPD), 2%, 5% and, 10%. The crystalline nature and the average crystallite size was studied by Powder XRD. Zinc doping was confirmed by EDAX. The TEM study indicated that pure and Zn doped CPPD nanoparticles were in the range from 4 nm to 40 nm. The presence of various bonds was confirmed by FT-IR spectroscopy. The amount of water of hydration and the thermal stability was studied by thermo-gravimetry. Formation of other phases on heating CPPD at 900 °C and 1250 °C were identified by the powder XRD. Substitution of Zn content significantly affects the crystallinity and thermal stability of nanoparticles. The results are discussed.

1 Introduction

With continuous advances in the field of implantable calcium phosphate based biomaterials have made impressive progress with regard to their biocompatibility and their ability to promote tissue formation [1]. Being similar to bone in composition and having bioactive properties, these materials are widely used as bone substitutes in dentistry and orthopedic applications [2]. Bioactive property is attributed to the surface composition and the structure of these bio-materials is similar to the mineral phase of bone. Other applications of calcium phosphates include repair of periodontal defects, sinus lifts, tooth replacement, spine fusion, ear and eye implants, and delivery systems of drugs [3]. A detailed review is written on this material by LeGeros [4]. Calcium pyrophosphate (CPP) – a shortest linear polyphosphate can also be used as a bone graft material [5]. Sintered dicalcium pyrophosphate (SDCP), a synthetic compound, has been proven to be more bio-compatible to bone tissue than hydroxyapatite [1]. Successive applications of these materials depend on the degree of bio-resorption, mechanical strength and bio-compatibility. Various factors such as chemical composition, physical characteristics and crystal structure affect the biological behavior of calcium phosphate materials [6]. In addition to that shape and size of the material plays an important role in the biological behavior of these materials [7]. Nano-size β-TCP (tri-calcium phosphate) has an advantage over micro size powders leading to increase mechanical properties and sinterability; in addition, its degradability can be regulated [8].

Influence of the inclusion of trace elements on the physical and/or chemical properties of the bio-ceramics has also been studied. Out of many trace elements, zinc is reported to be involved in bone metabolism. In case of bone-repairing, zinc improves the bone activity of osteoblast and promotes bone regeneration [9]. Apart from this, zinc is also an essential trace element in a variety of cellular processes including DNA synthesis, behavioral responses, bone formation, bone growth and wound healing [10]. Various divalent metal ions such as Zn, Sr, Mg, Mn and Tb doped TCP, hydroxyapatite, biphasic and calcium phosphate nanoparticles are well studied [11–17]. Recently, degradation and mineralization of calcium polyphosphate doped with various ions is reported [18]. Zn has a small ionic radius (0.074 nm) than calcium (0.099 nm) and based on the inter-atomic potential studies it might be thought to replace calcium in CPP with no dramatic effect on the structure [19].

The high surface-to-volume ratio present in nanoparticles is expected to alter its physical and chemical properties for different applications. Recently, calcium, manganese, cerium and titanium and cobalt -iron mixed pyrophosphate nanoparticles have been synthesized and well studied [20–23]. Looking at the applications of Zn doped calcium pyrophosphate as an important biomaterial, the present authors have synthesized pure and 2%,

[a] e-mail: sonalvasant@rediffmail.com

5% and 10%Zn doped CPPD nanoparticles by using surfactant mediated approach and characterized by EDAX, powder XRD, TEM, FT-IR and TGA. The effect of heating at different temperatures on the structure was studied by powder XRD.

2 Experimental technique

Surfactant mediated approach, discussed in detail elsewhere [24], was used to synthesize pure and Zn doped CPPD nanoparticles. The 0.5 M aqueous solutions of calcium nitrate tetra-hydrate ($Ca(NO_3)_24H_2O$) and $ZnCl_2$ were prepared in such a way that the [Zn]/[Ca] molar ratio varied as 0% (pure CPPD), 2%, 5%, 10%. The 0.25 M aqueous solution of sodium pyrophosphate ($Na_4P_2O_7$) was added in a drop-wise manner into the mixture of $Ca(NO_3)_24H_2O$, $ZnCl_2$ and surfactant with constant stirring at 50 °C. The water to surfactant ratio was maintained as 5:1. A non-ionic surfactant octoxynol 9 was used. The resulting precipitates were quickly filtered; washed with the deionized water and air dried. AR grade chemicals were used for the synthesis. The synthesized pure and Zn-CPPD nanoparticles were heated by placing them in ceramic crucibles in a muffle furnace. The samples were heated at 900 °C for one hour and samples were heated at 1250 °C for 15 min, where two different forms of calcium pyrophosphate, namely β-CPP and α-CPP, are found to be stable.

The powder XRD was carried out on Philips X'pert MPD system using Cu Kα radiation. The EDAX analysis was carried out on Philips ESEM EDAX XL-30. The TEM images were recorded on Philips-Tecnai using EHT potentials of 200 kV. The thermo-gravimetry was carried out using Netzsch Geratebau GmbH in the atmosphere of nitrogen from room temperature to 700 °C. The FT-IR spectra were recorded in KBr medium using Thermo-Nickolet 6700 set up in the range from 400 cm^{-1} to 4000 cm^{-1}.

3 Results and discussion

3.1 Powder XRD

The powder XRD was carried out to study the crystalline nature of the nanoparticles and to estimate the average crystallite size. Figure 1a shows the powder XRD patterns for pure and Zn doped CPPD nanoparticles. The peak broadening in XRD pattern of pure CPPD reflects the nano-crystalline nature of the sample. The powder XRD data were analyzed by computer software Powder-X. The triclinic system was found with unit cell parameters as, $a = 7.365$ Å, $b = 8.287$ Å, $c = 6.691$ Å, $\alpha = 102.96°$, $\beta = 72.73°$ and $\gamma = 95.01°$, which corresponds to that of the reported in the literature [25]. From Figure 1a, one can notice that the addition of small molar percentage of Zn affects the crystallinity in significant manner; the crystallinity of non-calcined Zn-CPP are found to be low since the diffraction peaks of the doped samples exhibit

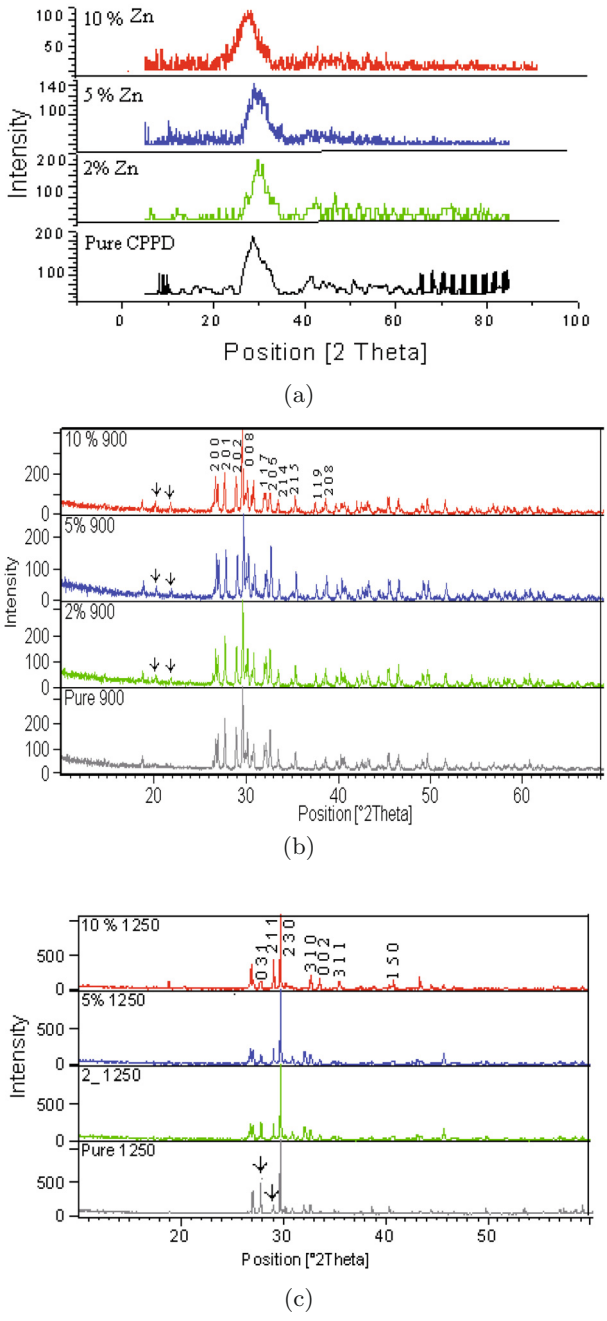

Fig. 1. (Color online) (a) XRD pattern of pure and Zn doped CPPD nanoparticles, (b) XRD pattern of 900 °C heated CPP nanoparticles and (c) XRD pattern of 1250 °C heated CPP nanoparticles.

comparatively low intensity, relatively broad and more distorted nature than pure CPPD nanoparticles. This result is in good agreement with the result obtained by Stanic et al. [26], LeGeros et al. [27] and Ren et al. [28] for hydroxyapatite nanoparticles. Substitution of Zn in calcium phosphate markedly reduces the crystallite size and, therefore, causes a reduction of crystallinity which is well studied [29,30]. Usually, the isomorphic substitutions of

different size of ions in the lattice of calcium phosphate based bio-materials are expected to disturb the crystalline distances among the constituent atoms, as a result it is often observed by the changes in the lattice parameters and in terms of the shift of the XRD peaks. Nevertheless, the perturbation of the structure depends on the doping amounts and on the size differences of the ions involved. In any case, a certain trend towards less sharp XRD peaks is expected. Masala et al. [19] have reported this nature for Zn doped CPP, in terms of the relative stability of the complexes formed by Zn and Ca with pyrophosphate. As binding constant of Zn in aqueous solution is 8.7 and it is 6.8 for Ca, therefore, Zn can compete with Ca for binding pyrophosphate even at a very low concentration and this results in decreased crystallinity [19], whereas, some authors [18] have explained on the basis of the difference in ionic radii of calcium (0.099 nm) and zinc (0.074 nm). Based on crystal structure theory one can expect that if the radii of doped ions are much smaller, it is easy to fill them in the vacancy or interstitial sites of crystal lattice presenting as interstitial solid solution, but these doped ions in an interstitial sites force the crystal to lose certain electric charges needed to maintain its electric neutrality, which causes equivalent charge ions to disengage and creates more vacancies for point defects [18]. Recently, it is reported that low crystalline material has higher bioactivity, which is favorable to its nano-bio-effects [14]. Figures 1b and 1c exhibit the powder XRD patterns of heated nanoparticles samples of pure and Zn doped CPPD at 900 °C and 1250 °C, respectively. Heated samples show sharper peak than those of as prepared samples, which indicates larger crystallite size and higher degree of crystallinity. This result is consistent with the theory that the particle size is proportional to crystallinity. Scherrer's formula was used to calculate the average crystallite size for pure CPPD and it is found to be 4 nm, 76 nm, 119 nm for as synthesized nanoparticles, 900 °C and 1250 °C heated samples, respectively.

It can be noticed from Figure 1b that, for pure CPPD heated samples at 900 °C, all the reflections of β-CPP are present. Tetragonal system was identified with unit cell parameters $a = b = 6.684$ Å, $c = 24.145$ Å (JCPDS No. 20-0024) [31]; whereas, the doped CPPD showed additional reflections and alterations in the intensity of some calcium pyrophosphate peaks. The additional low intensity peaks around 21.543° ($d = 4.12$) and 24.90° ($d = 3.57$) (marked with small arrows in figure) are observed, which are due to (−1 −1 1) and (−1 −1 2) reflections of $CaZn_2(P_2O_4)_2$ (JCPDS No. 84-1569) [32] and the strongest reflection at 29.680° ($d = 3.01$) due to (0 1 2) plane of $CaZn_2(P_2O_4)_2$ is overlapped by (0 0 8) reflection of β-CPP.

Figure 1c shows the XRD pattern of the sample heated at 1250 °C, which shows all the characteristic reflections of α-CPP with orthorhombic structure (JCPDS No. 09-0345) [33]. The intensity of reflection at 29.677° ($d = 3.01$) (indicated by small arrow in figure) due to (2 3 0) is found to be increased with increase in doping concentration, which is the characteristic peak of $CaZn_2(P_2O_4)_2$ as described earlier in the previous paragraph.

Table 1. Atomic and weight % of Zn obtained through EDAX.

Sample	Atomic %	Weight %
2%Zn doped CPPD	0.34	1.09
5%Zn doped CPPD	0.58	1.98
10%Zn doped CPPD	1.32	4.40

Table 2. Remaining weight percent at 100 °C and 600 °C obtained from thermo-grams.

Sample	Remaining weight % at 100 °C	Remaining weight % at 600 °C
Pure	92.32	66.87
2%Zn doped CPPD	87.98	81.43
5%Zn doped CPPD	91.51	84.63
10%Zn doped CPPD	94.67	87.56

The intensity of α-CPP characteristic peak at an angle 26.696° ($d = 3.30$) due to (0 3 1) reflection is found to be decreased with increase in doping concentration.

3.2 EDAX analysis

The EDAX analysis was carried out to confirm the Zn doping. It showed that the doped samples were composed of calcium, phosphorous and oxygen with a small percentage of Zinc. The amount of Zn increased as the [Zn]/[Ca] molar ratio increased, which ensured that the doping was achieved successfully. Table 1 shows the atomic percent and weight percent of Zn obtained for doped samples by using this analysis.

3.3 TEM analysis

The TEM analysis was carried out to confirm the particle size and morphology of the samples. The pure and Zn doped samples showed the variation of particle size from 4 nm to 40 nm. The particle size was not affected by the amount of Zn doping. Figures 2a and 2b shows the TEM images of pure and 10%Zn doped CPPD nanoparticles, respectively, which shows nearly spherical morphology.

3.4 TGA analysis

The TGA analysis was carried out to find out the thermal stability of the samples. Figures 3a and 3b shows the thermo-grams of pure CPPD nanoparticles and 2%Zn doped CPPD nanoparticles. On heating, the samples started loosing their thermal stability by giving up water molecules and achieved the anhydrous states over 300 °C and remained stable up to the end of the analysis. Table 2 gives the values of remaining weight percent at 100 °C and 600 °C, it is found to be increased as the doping concentration increased. The stability was increased as zinc content increased in the CPPD nanoparticles. This may be due to the decrease in the lattice energy on substitution

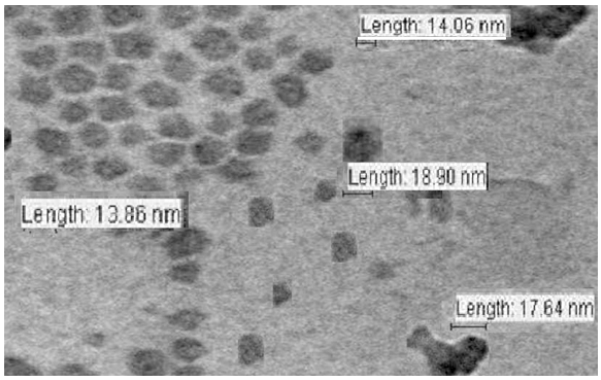

(a)

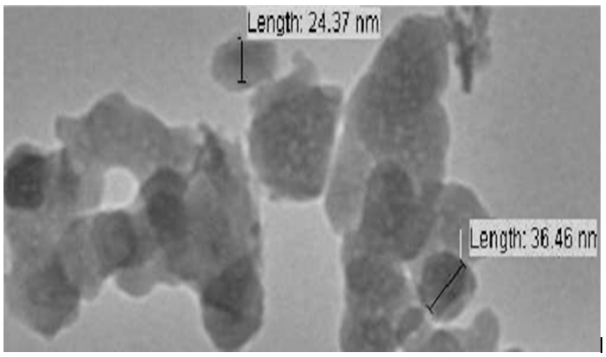

(b)

Fig. 2. (a) TEM image of pure CPPD nanoparticles and (b) TEM image of 10%Zn doped CPPD nanoparticles.

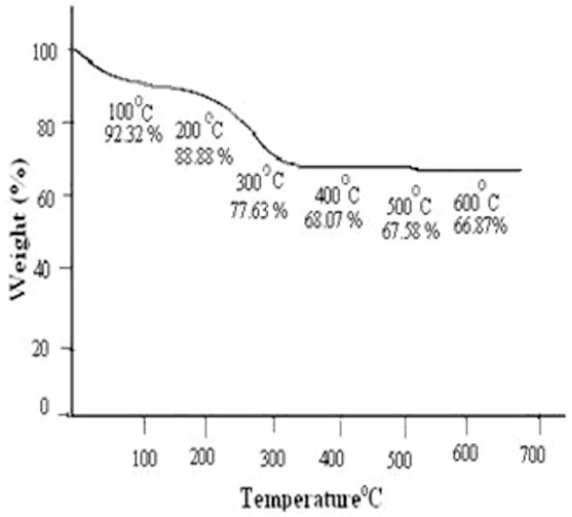

(a)

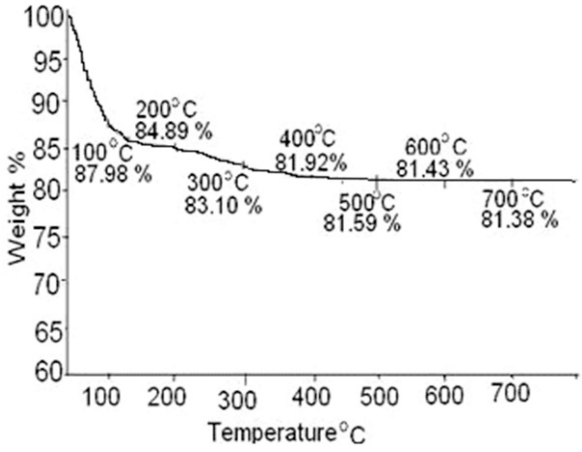

(b)

Fig. 3. (a) Thermo-gram of pure CPPD nanoparticles and (b) thermo-gram of 2%Zn doped CPPD nanoparticles.

of Zn in CPPD giving stabilizing effect, which corresponds to the results obtained by Simkiss and Taylor [34]. It was found that pure and Zn doped samples were containing two water molecule associated with them.

3.5 FT-IR spectroscopy

The FT-IR spectroscopy was carried out to confirm the bonds present in the samples. Figure 4a shows the FT-IR spectra of pure and doped CPPD. In all spectra, the similar bands are present, though, with increased transmittance values as doping concentration increases. This can be attributed to the small variations in the sample surface composition [35]. The broad absorption occurring at 3417.5 cm^{-1} is due to -OH stretching vibration, which supports the result obtained from TGA that all samples contain water molecules. The absorption observed at 1645.3 cm^{-1} is attributed to O-H plane bending. As the strength of P-O bond in the P-O-P bridge is weaker than in the $(PO_2)^{2-}$ radical, the stretching frequencies of the P-O-P bridge are expected to be lower than those in the $(PO_2)^{-2}$ radical. The asymmetric and symmetric stretching frequencies of the $(PO_2)^{2-}$ radical are generally observed in the frequency areas 1100–1000 cm^{-1}, 1000–900 cm^{-1}, respectively; in the present investigation it is observed around 1136.9 cm^{-1} and 924.7 cm^{-1}, respectively, for pure CPPD [21]. Asymmetric P-O-P bridge vibration is observed at 740.7 cm^{-1}. Metal-oxygen stretching vibration is observed at the 563.9 cm^{-1}. Figure 4b shows the FT-IR spectra of pure CPPD samples recorded after heating at 900 °C and 1250 °C and compared with as synthesized nanoparticle samples. The broadening of the absorption bands disappears in the FT-IR spectra of the sample heated at 900 °C and 1250 °C, which shows the effect of crystallite size on the absorption in FT-IR spectra.

4 Conclusions

Pure and doped CPPD nanoparticles were synthesized using surfactant mediated approach. The peak broadening in powder-XRD pattern of pure CPPD nanoparticles suggested the nano-structured nature with triclinic system and the average particle size was estimated to be 4 nm

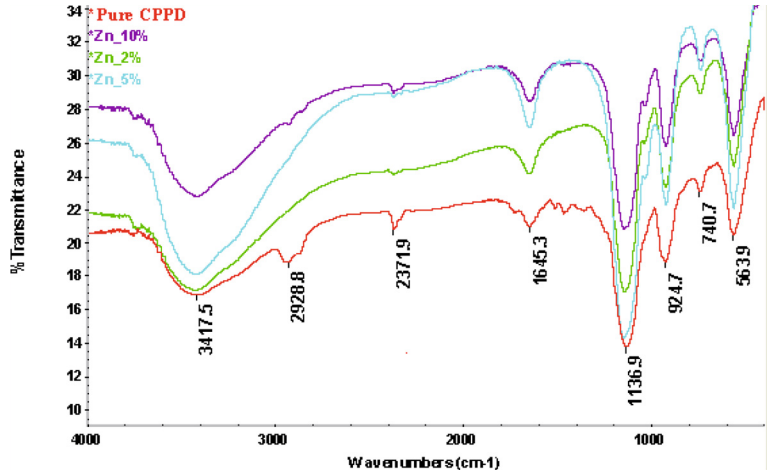

(a)

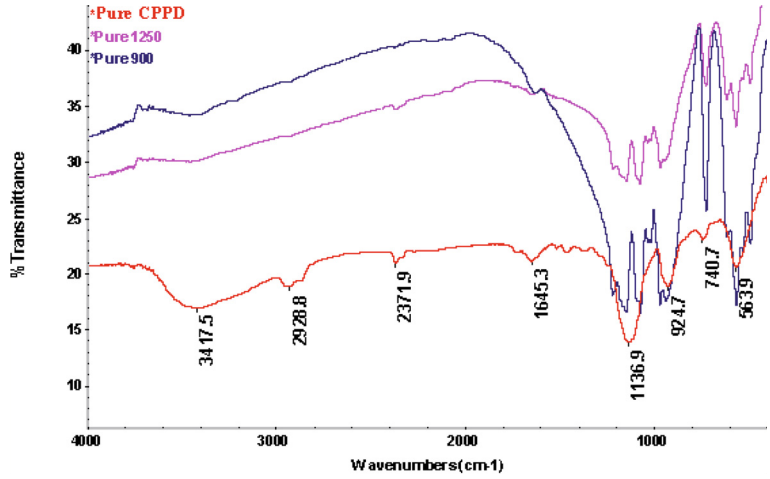

(b)

Fig. 4. (Color online) (a) FT-IR spectrum of pure and doped CPPD nanoparticles. (b) FT-IR spectrum of pure and heated CPPD nanoparticles.

by applying Scherrer's formula and it was found to be 76 nm and 119 nm for 900 °C and 1250 °C heated CPPD nanoparticles, respectively. Crystallinity was found to be decreased with increasing the zinc doping concentration. The TEM confirmed that the particles were of spherical morphology and the particle size varied between 4 nm to 40 nm, which was not affected by amount of dopant. Heating of pure CPPD nanoparticles at 900 °C and 1250 °C temperatures in a furnace yielded β-CPP and α-CPP phases of CPP, respectively, which was confirmed by the Powder XRD; whereas the doped samples showed additional reflections of $CaZn_2(P_2O_4)$. The FT-IR study confirmed the presence of pyrophosphate, metal-oxygen and O-H bond in the structure. The nano-structured nature of the samples introduced broadening in the absorption bands in the FT-IR spectra of non-calcined samples. TGA confirmed the dihydrate form of CPP and higher stability of pyrophosphate compound. Substitution of Zn content significantly affects the crystallinity and thermal stability.

The author (S.R. Vasant) is thankful to the UGC, New Delhi, for the UGC-JRF under the meritorious student's scheme. The authors are thankful to Government of Gujarat for giving financial assistance under the sanctioned project on "Nanoscience and Technology and Environmental Physics", and Prof. K.N. Iyer (Saurashtra University) for his keen interest. The authors are also thankful to Prof. J.M.F. Ferreira, Averio, Portugal for discussion and valuable suggestion on XRD.

References

1. J.S. Sun, Y.H. Tsuang, C.J. Liao, H.C. Liu, Y.S Hang, F.H. Lin, J. Biomed. Mater. Res. **37**, 324 (1997)
2. C.G. Simon Jr., J.M. Antonucci, D.W. Liu, D. Skrtic, J. Bioact. Compat. Polym. **20**, 279 (2005)
3. W. Paul, C.P. Sharma, Trends Biomater. Artif. Organs **19**, 7 (2005)
4. R.Z. LeGeros, Chem. Rev. **108**, 4742 (2008)

5. J.H. Lee, D.H. Lee, H.S. Ryu, B.S. Chang, K.S. Hong, C.K. Lee, Key Eng. Mater. **240**, 399 (2003)
6. S.R. Radin, P. Ducheyne, J. Biomed. Mater. Res. **28,** 1303 (1994)
7. N.K. Wood, E.J. Kaminski, R.J. Oglesby, J. Biomed. Mater. Res. **4**, 1 (1970)
8. K. Lin, J. Chang, J. Lu, W. Wu, Y. Zeng, Ceram. Int. **33**, 979 (2007)
9. W.J. Bettger, B.L. O'Dell, J. Nutr. Biochem. **4**, 194 (1993)
10. D.G. Barceloux, J. Toxicol. Clin. Toxicol. **37**, 279 (1999)
11. M. Li, X. Xiao, R. Liu, C. Chen, L. Huang, J. Mater. Sci.: Mater. Med. **19**, 797 (2008)
12. S.J. Kalita, M. Ferguson, Am. J. Biochem. Biotechnol. **2**, 57 (2006)
13. S. Gomes, G. Renuaudin, E. Jallot, J.M. Nedelec, Appl. Mater. Interfaces **1**, 505 (2009)
14. X. Cao, F. Wen, W. Bian, Y. Cao, S. Pang, W. Zhang, Front. Mater. Sci. China **3**, 255 (2009)
15. I. Soyapan, A.N. Natasha, Ionics **9**, 330 (2009)
16. A. Cuneyt Tas, S.B. Bhaduri, S. Jalota, Mater. Sci. Eng. C **27**, 394 (2007)
17. Y. Han, X. Wang, S. Li, X. Ma, J. Sol-Gel Sci. Technol. **49**, 125 (2009)
18. W. Song, M. Tian, F. Chen, Y. Tian, C. Wan, X. Yu, J. Biomed. Mater. Res. **89**, 430 (2009)
19. O. Masala, P. O'Brien, G. Rafeletos, Cryst. Growth Des. **3**, 431 (2003)
20. S.R. Vasant, M.J. Joshi, Mod. Phys. Lett. B **24**, 1 (2010)
21. B. Boonchom, R. Baitahe, Mater. Lett. **63**, 2218 (2009)
22. W. Wenwei, F. Yanjin, W. Xuehang, L. Sen, H. Xiufu, L. Xuanhai, Rare Met. **28**, 33 (2009)
23. B. Boonchom, N. Phuvongpha, Mater. Lett. **63**, 1709 (2009)
24. M. Uota, H. Arakawa, N. Kitamura, T. Yoshimura, J. Tanaka, T. Kijima, Langmuir **21**, 4724 (2005)
25. G.S. Mandel, K.M. Renne, A.M. Kolbach, W.D. Kalpan, J.D. Miller, N.S. Mandel, J. Cryst. Growth **87**, 453 (1988)
26. V. Stanic, S. Dimitrijevic, J. Antic-Stankovic, M. Mitric, B. Jokic, I.B. Plecas, S. Raicevic, Appl. Surf. Sci. **256**, 6083 (2010)
27. R.Z. LeGeros, M.M. Taheri, G.B. Quirologico, J.P. LeGeros, in *Proc. of the 2nd Int. Phosphorus Conf., Boston* (IMPHOS, Paris, 1989), pp. 89–103
28. F. Ren, R. Xin, X. Ge, Y. Leng, Acta Biomater. **5**, 3141 (2009)
29. A.M. Costa, G.A. Soares, R. Calixto, A.M. Rossi, Key Eng. Mater. **256**, 119 (2004)
30. F. Miyaji, Y. Kono, Y. Suyama, Mater. Res. Bull. **40**, 209 (2005)
31. N.C. Webb, Acta Crystallogr. **21**, 942 (1966)
32. R.J.B. Jakeman, A.K. Cheetham, Am. Chem. Soc. **110**, 1140 (1988)
33. W.L. Hill, G.T. Faust, D.S. Reynolds, Am. J. Sci. **242**, 457 (1944)
34. K. Simkiss, M.G. Taylor, J. Exp. Biol. **190**, 131 (1994)
35. J.R. de Lima, A.M. Costa, I.N. Bastos, J.M. Granjeiro, G. de A. Soares, Mater. Res. **9**, 399 (2006)